Mechanical properties and structure formation amorphous of $Zr_{59}Ta_5Cu_{18}Ni_8Al_{10}$ bulk metallic glass alloy

B. Bendjemil[1,2,3*], A. Hafs[1], N. Seghairi[4], M. Baricco[1]

[1] *Dipartimento di Chimica, Università di Torino, Via P. Giuria 9, 10125 Italy*
[2] *LEREC, University of Badji Mokhtar, P. Box 12, 23000. Annaba, Algeria*
[3]*University of Guelma, P. Box 12, 24000, Guelma, Algeria*
[4]*Faculty of Sciences and Engineering, University of Oum El-Bouaghi, Algeria*

Abstract

In the present paper thermal stability and structure of $Zr_{59}Ta_5Cu_{18}Ni_8Al_{10}$ (numbers indicate at. %) glassy alloys were investigated. The structural studies revealed an amorphous structure for the rod with a diameter of 2 mm was prepared through water-cooled copper mold casting and in a ribbon form by the single roller melt-spinning method. The obtained results confirm the utility of applied investigation methods in the thermal and structure analysis of examined amorphous alloys. The thermal properties associated with crystallization temperature of the glassy samples were measured using differential thermal analysis and differential scanning calorimetry. The microstructure and constituent phases of the alloy composite have been analyzed by using X-ray diffraction. Mechanical property of bulk $Zr_{59}Ta_5Cu_{18}Ni_8Al_{10}$ alloy with a diameter 2 mm measured by compression tests at room temperature and morphologies of the fractured observed by Scanning Electron Microscopy (SEM). The Energy Dispersive Spectrometer (EDS) micro-analysis is performed by measuring the energy and intensity distribution of X-ray signals generated by a focused electron beam on the specimen.

1. Introduction

Since the pioneering work of Inoue and coworkers [1] on bulk metallic glasses (BMGs), a large number of metallic systems with high glass forming ability have been developed [2]. Among the various systems, Zr-based BMGs are of particular interest because of the positive combination of remarkable mechanical, physical and chemical properties, which largely enhances the possibility of industrial applications [3].

BMGs are generally produced by solidification techniques (e.g. melt spinning and copper mold casting), where the high cooling rate applied permits to bypass nucleation and growth of the stable crystalline phase and to produce a metallic glass [4].

---

[*]) For correspondence, Mobile: 06 97 28 07 56. E-mail: bendjemilbadis@yahoo.fr

Although Zr-based BMGs with a critical cooling rate as low as $1–100 \mathrm{Ks}^{-1}$ [5] sufficient to obtain high levels of under-cooling and produce fully glassy rods with diameters ranging from 5 to 10 cm [7] have been developed, typical critical dimensions for Zr-based glasses are of the order of few millimeters [5].

Crystallization studies on the metallic glasses play a vital role in the area of amorphous alloys [6]. Controlling the microstructure development from the glassy precursors requires detailed understanding of the specific mechanisms influencing structural transformations [7], helping in producing structure specific components. Moreover, crystallization studies are essential for the proper choice of the consolidation parameters (i.e. consolidation time and temperature) in order to maximize densification and, at the same time, avoiding the crystallization of the material [8].

At the present time, metal glasses are already used for their particular mechanical properties in a certain number of applications such as articles of sport (club of golf, rackets of tennis, and beaters of baseball) which exploit their aptitude to restore elastic energy, associated with a weak dissipation.

The aim of the present work is to study the glass formation behavior of the $Zr_{59}Ta_5Cu_{18}Ni_8 Al_{10}$ prepared by the melt-spinning process, in the ribbon shape, and then injected into a copper mould to prepare alloy rods of about 2 mm in diameter. The mechanical properties of the composite have been examined through compression tests and indentation fracture of amorphous alloy is presented.

2. Experimental

An ingot of the $Zr_{59}Ta_5Cu_{18}Ni_8 Al_{10}$ alloy (composition is given in nominal atomic percentages) was prepared by arc-melting mixtures of Zr 99.99 mass% purity, Ta 99.8 mass% purity, Cu 99.9 mass% purity , Ni 99.9 mass% purity and Al 99.9 mass% purity in an argon atmosphere purified using Ti-gettering. In order to obtain a master alloy, followed by induction melting the master alloy and injection casting into a water-cooled copper mold to form 50 mm long cylinders with diameters of 2 mm. For comparison, thin ribbons of 5 mm width and about 30 μm thickness was prepared using a single-roller, melt spinning technique under a vacuum atmosphere.

All the ribbons and cylinders were investigated by differential scanning calorimetry (DSC) using a constant heating rate of 10°C /mn. The structure of the samples was examined by X-ray diffraction (XRD) with Cu Kα ($\lambda = 1.54056 \text{Å}$) radiation and energy dispersive Spectrometer (EDS). Scanning electron microscopy ((JEOL JSM6400F) was employed for the analysis of the fracture features. The compression properties were tested by using an Instron testing machine at a strain rate of $5 \times 10^{-4} \text{s}^{-1}$ at room temperature.

3. Results and Discussion

Figure 1 shows the constant-rate heating (10°C/mn) DSC curves of $Zr_{59}Ta_5Cu_{18}Ni_8 Al_{10}$ analysis was carried out for melt-spun ribbons and as-cast cylinders. In the temperature range investigated, all the curves are characterized by two exothermic peaks, revealing a multi-step crystallization path that does not depend on the method of preparation. The analysis of the thermal stability data, summarized in Table 1, reveals striking similarities between the as-cast cylinders and the melt-spun ribbon.

Table 1: Summary of the glass transition temperature Tg, crystallization temperature T_{x1}, T_{x2}, and supercooled temperature region ΔT_x for the melt-spun ribbons and as-cast rod 2 mm (continuous heating at10°C/mn)

Temperatures	Melt-spun ribbon	as-cast rod 2 mm
T_g (°C)	343	342
T_{x1}(°C)	402	400
T_{x2}(°C)	431	430
ΔT_x(°C)	59	58

The DSC curves indicate a small difference in glass transition temperature (Tg), crystallization temperature (Tx), supercooled liquid region (ΔTx = Tx −Tg) between the ribbon and rod samples, for the as cast 2 mm-diameter cylinder shows that alloy presents two over-lapping exothermic peak around 400 - 430 (°C). The glass transition temperature, Tg, is 342 (°C). The melt-spun ribbon for the same alloy presents two exothermic peaks corresponding to two distinct stages of phase transformations $T_{x1}$and Tx$_2$ 402,431(°C), respectively   and an obvious Tg is 343 (°C).

In order to confirm the glassy state of the samples, further X-ray diffraction measurements were performed. Figure 2 shows XRD pattern of the cast $Zr_{59}Ta_5Cu_{18}Ni_8 Al_{10}$ rod with a diameter of 2 mm, together with the XRD pattern of the melt-spun glassy alloy ribbon. Only a broad peak is seen around a diffraction angle of 39° for the bulk sample and ribbon, no detectable sharp diffraction peak indicating crystalline structure can be observed. These are typical XRD patterns of amorphous structures, confirming that both samples possess amorphous structures [9].
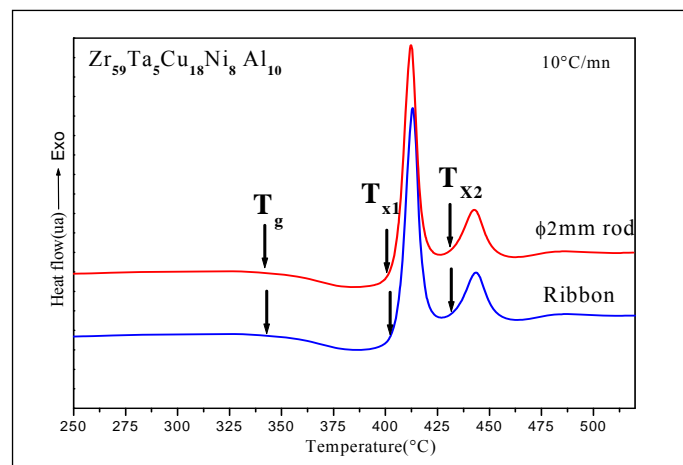

Figure 1: DSC curves of $Zr_{59}Ta _5Cu_{18}Ni_8 Al_{10}$ alloy ribbon and rods with diameters of 2mm.

The critical cooling rate for glass formation, Rc, is an important characteristic parameter for predicting the ease or difficulty of glass formability. It is defined as the minimum cooling rate necessary to keep the melt amorphous without detectable crystallization upon solidification. A slower Rc indicates a greater glass-forming ability of an alloy system. By considering the liquid-solid transformation behavior under non-isothermal conditions, Barandiaran and Colmenero [10] obtained a relation which enables Rc to be estimated directly fromthermal analytical measurements.
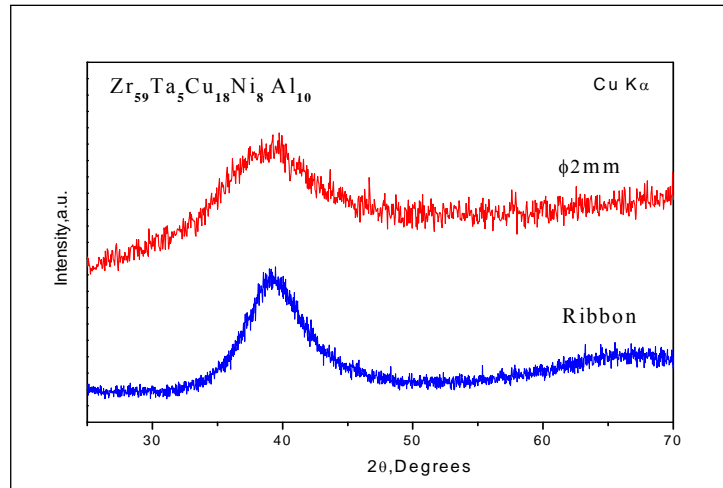
Figure 2: XRD pattern of the cast $Zr_{59}Ta_5Cu_{18}Ni_8Al_{10}$ rod with a diameter of 2 mm, together with the XRD pattern of the melt-spun glassy alloy ribbon.

Figure 3 shows the compressive stress–strain curve at a strain rate of 5×10^{-4} s^{-1}. The fracture of the samples occurs at a fracture stress σf of 2041MPa and elastic a deformation up to a strain of about 2.13 followed by a small compressive plastic strain in the range of 2.13 -2.24.Young's modulus is determined as 95 GPa for the 2 mm diameter sample.
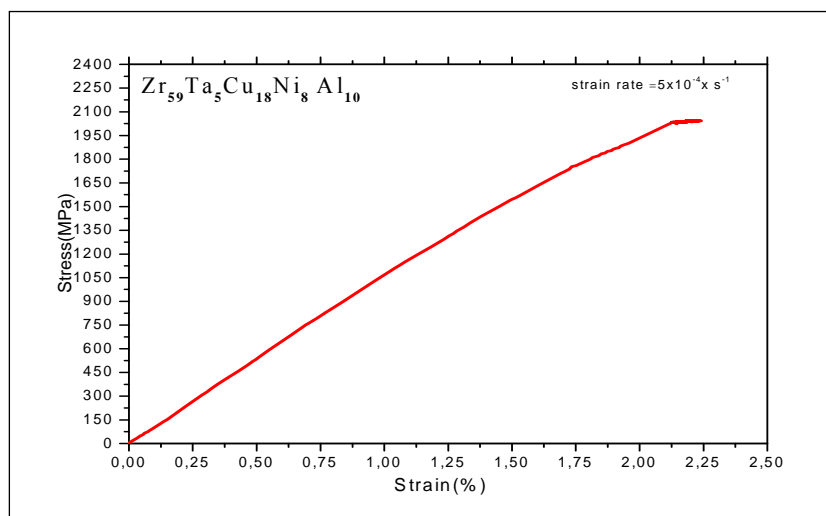

Figure 3: Compressive stress–strain curves of cast $Zr_{59}Ta_5Cu_{18}Ni_8Al_{10}$ glassy alloy rods under an niaxial compression testing at room temperature.

A significant strengthening composites with nanostructured matrix [11] can act as obstacle to restrict the excessive deformation of the matrix avoiding catastrophic failure. The dendritic phase is a rather soft phase and contributes to the plasticity by inducing dislocations in the materials. For present $Zr_{59}Ta_5Cu_{18}Ni_8Al_{10}$ alloy, the as-cast intermetallic precipitates do not decrease the fracture strength (2041MPa) because of the existence of the ductile dendrites. This indicates that the ductile dendrites act as obstacles to prevent brittle failure of the materials. For the 2 mm diameter sample, the mechanical properties are extremely deteriorated as shown in Figure 3. This is believed to be attributed to the larger volume fraction [12] and coarser grain size [13] of the intermetallic precipitates in the 2 mm diameter samples due to the lower cooling rate during casting. The Young's modulus is determined as 95GPa for the 2 mm diameter sample, which is larger than those of the

$Zr_{65}A_{l7.5}Ni_{10}Cu_{17.5-x}Ag_x$ (x=5 and 10 at.%) BMGs, but is comparable to that of the annealed $Zr_{65}A_{l7.5}Ni_{10}Cu_{12.5}Ag_5$ alloy containing approximately 85% nanometer scaled I-phases [13] and $Zr_{58}Al_9Ni_9Cu_{14}Nb_{10}$ alloy containing 90% quasicrystal. The elasticity is several times superior than that of $Al_{63.5}Cu_{24.5}Fe_{12}$ and $Al_{70}Pd_{20}Mn_{10}$ poly-crystalline icosahedral quasicrystals [15], while the measured Young's modulus value is much lower than those of the conventional quasicrystals as shown in Table 2.

Table 2: Mechanical properties of the present materials compared with Al- and Zr-based non-crystalline alloys

Materials	Phase constituents	Elastic stress limit σ_f (Mpa)	Elastic deformation limit ε_e (%)	Young's modulus E (GPa)
$Al_{70}Pd_{20}Mn_{10}$ [16]	I-phase	520 (fracture)	0.3	200
$Al_{63}Cu_{25}Fe_{12}$ [17]	I-phase	250 (fracture)	0.35	172 [18]
$Zr_{65}A_{l7.5}Ni_{10}Cu_{12.5}Ag_5$ [19]	BMGs	1650 (fracture)	1.95	84.5
$Zr_{65}A_{l7.5}Ni_{10}Cu_{12.5}Ag_5$ [19]	85% quasicrystal +15% glass	1200 (fracture)	1.5	90
$Zr_{58}Al_9Ni_9Cu_{14}Nb_{10}$ [20]	90% quasicrystal +10% glass	1800 (fracture)	2.0	92
$Zr_{59}Ta_5Cu_{18}Ni_8 Al_{10}$ (this work)	BMGs	2041(fracture)	2.13	95

The appearance of the fracture surface was investigated by SEM. Figure 4(a and b) show micrographs of the $Zr_{59}Ta_5Cu_{18}Ni_8 Al_{10}$ as-cast rectangular bar after fracture at different magnifications. Figure 4(a) shows a side view of the fractured sample. There are no distinct veins and dimples, at least not over the whole fracture surface but only in some regions. For the sample studied here, the fracture surface appears to consist of a high number of small fracture zones, which leads to breaking of the samples into many small parts, as indicated in Figure 4(b).

The results of chemical analysis of the $Zr_{59}Ta_5Cu_{18}Ni_8 Al_{10}$ rod with a diameter 2 mm by EDS [21] attached to SEM was show on Figure 5.

The structural evolution during heating was investigated by XRD. The diffraction patterns of rod form with diameter of 2 mm at prepared through water-cooled copper mold casting heated to different temperatures are shown in Figure 6 of the $Zr_{59}Ta_5Cu_{18}Ni_8 Al_{10}$ glassy alloy that is subjected to annealing for 9 min at different annealing temperature. The rod form with diameter of 2 mm broad maxima characteristic for amorphous materials and no trace of crystalline phases, indicating that they are in the amorphous state for temperatures between 200°C and 350°C.for $Zr_{59}Ta_5Cu_{18}Ni_8 Al_{10}$ The phase formation reflects at the T=350°C and 400°C. Obviously, the first step of devitrification is mostly linked with the formation of quasicrystalline phase, in the figures 6. Concerning XRD patterns of the bulk samples in $Zr_{59}Ta_5Cu_{18}Ni_8 Al_{10}$ at 450 °C are identified the crystalline phases after complete crystallization of the as-cast 2 mm include Zr_2Cu , Zr_2Ni and Zr_2Al . Further study shows that there is similar tendency of the microstructure as the holding time increases from 3 to 9 min at 450 C.
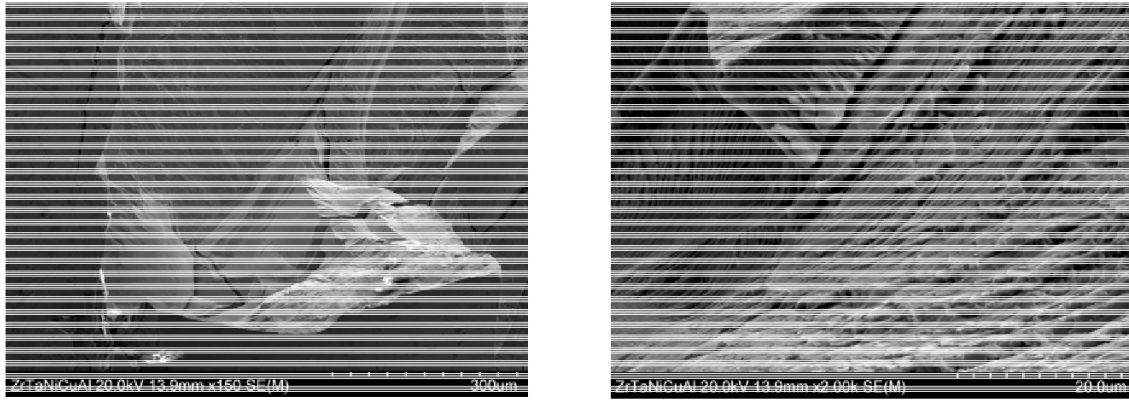
Figure 4: SEM micrographs of the fracture morphology of $Zr_{59}Ta_5Cu_{18}Ni_8 Al_{10}$ amorphous rod in as −cast state with diameter of 2 mm (a) shows a side view of the fractured sample; (b) the higher magnification image showing the typical characteristics of a fracture.
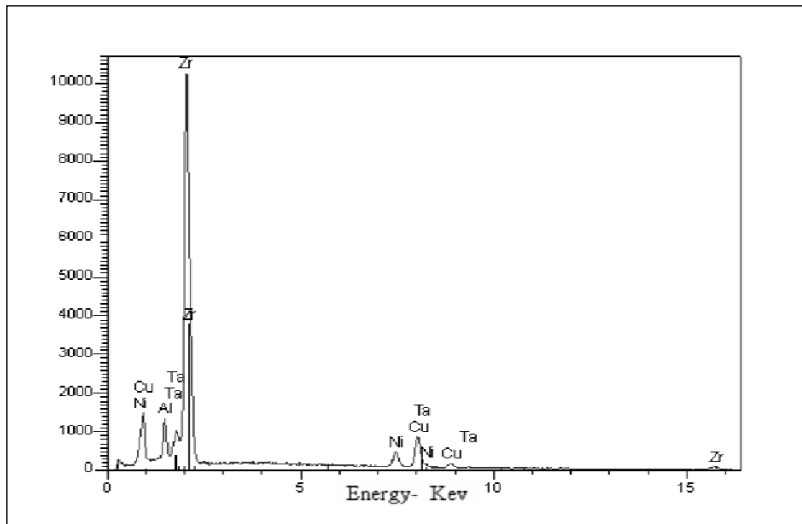

Figure 5: Energy dispersive spectra of the $Zr_{59}Ta_5Cu_{18}Ni_8 Al_{10}$ alloy.
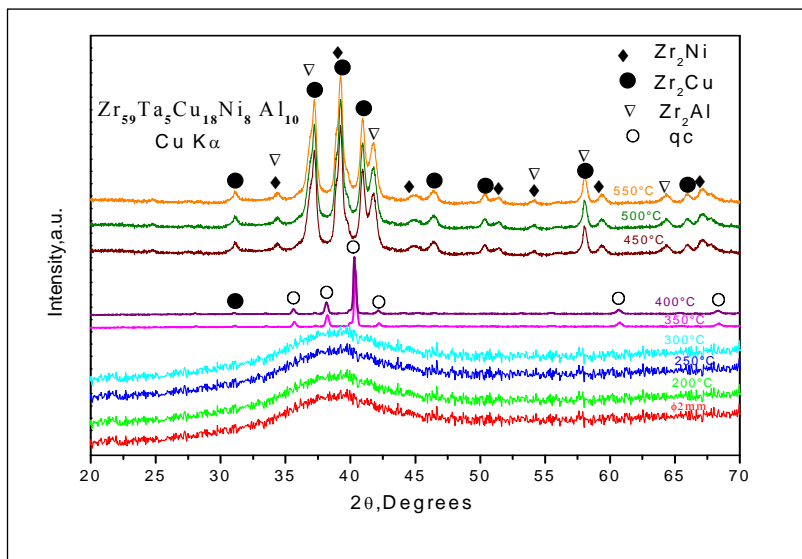

Figure 6: XRD scans of annealed sample of $Zr_{59}Ta_5Cu_{18}Ni_8 Al_{10}$ alloy of rod form with diameter of 2 mm.

4. Conclusion

In conclusion, The comparison between the ribbon were obtained directly from the melt-spinning technique and the same alloy produced by injection casting of the molten alloy into copper moulds with cylindrical cavities reveals that both types of samples are characterized by the formation phase amorphous obtained in X-ray diffraction . The bulk glassy rods possess good mechanical properties, the compressive fracture strength and elastic strain to fracture of the amorphous alloy with 2, 13 at. % also exhibit ultrahigh fracture strength of 2041MPa, Young's modulus of 95 GPa. The stable crystalline phases include Zr_2Cu, Zr_2Ni and Zr_2Al after complete crystallization of the as-cast 2 mm at 450°C.

Acknowledgement

References

[1]   T. Zhang, A. Inoue, T. Masumoto, Mater. Trans. JIM **32** (1991) 10005

[2]   J. Basu, S. Ranganathan, Sadhana **28** (2003) 783

[3]   M. Telford, Mater. Today **7** (2004) 36

[4]   W. L. Johnson, MRS Bull. **24** (1999) 42

[5]   Y. J. Kim, R. Busch, W. L. Johnson, A. J. Rulison and W. K. Rhim, Appl. Phys. Lett., **65** (1994) 2136

[6]   J. F. Löffler, Intermetallics, **11** (2003) 529

[7]   J. H. Perepezko, Prog. Mater. Sci., **49** (2004) 263

[8]   P. Yu, K. B. Kim, J. Das, F. Baier, W. Xu, J. Eckert, Scripta Mater. **54** (2006) 1445

[9]   A. Bouchareb, B. Bendjemil, R. Piccin, M. Baricco. Int. J. Nanoelectronics and Materials **3** (2010) 63-70

[10] J. M. Barandiaran, J. Colmenero, J. Non-Cryst. Solids **46** (1981) 277

[11] G. He, Z. F. Zhang, W. Löser, J. Eckert, L. Schultz. Acta Materialia **51** (2003) 2383

[12] G. He, W. Löser and J. Eckert, Scripta Materialia **48** (2003) 1531

[13] He. G, Lu. J, Bian. Z, Chen. DJ, Chen. GL, Tu. GC and Chen. G, J. Engineering, Computing & Technology **42** (2001) 356

[14] M. F. Ashby and A. L. Greer, Scripta Mater., **54** (2006) 321

[15] Q. J. Chen, J. Shen, D. L. Zhang, H. B. Fan and J. F. Sun, J. Mater. Res. **22** (2007) 358

[16] Koster U, Liebertz H, Liu W. *International Conference on Rapidly Quenched and Metastable Materials* N°8, Sendai, JAPON (22/08/1993) 1994, vol. 181-82 (15 ref.), pp. 777-780.

[17] Vanderwal JJ, Zhao P, Walton D. Phys Rev., B**46** (1992) 501

[18] A. Inoue, T. Zhang, M. W. Chen, T. Sakurai, J. Saida and M. Matsushita. Journal of Materials Research, **15** (2000) 2195

[19] J. B. Qiang, W. Zhang , Guoqiang Xie, Hisamichi Kimura, C. Dong, A. Inoue. Intermetallics **15** (2007) 1197

[20] Z. F. Zhang, G. He, J. Eckert and L. Schultz, Phys. Rev. Lett., **91** (2003) 045505

[21] B. Bendjemil, N. Seghairi, A. Bouchareb, A. Hafs, M. Barrico. Int. J. Nanoelectronics and Materials **3** (2010) 35